A drifting GPS buoy for retrieving effective riverbed bathymetry.

R. Hostache[a,*], P. Matgen[a], L. Giustarini[a], F.N. Teferle[b], C. Tailliez[a], J.-F. Iffly[a], G. Corato[a]

[a] *CRP-Gabriel Lippmann, 41 rue du Brill, L-4422 Belvaux, Luxembourg.*
[b] *University of Luxembourg, Faculté des Sciences, de la Technologie et de la Communication, 6 rue Richard Coudenhove-Kalergi, L-1359 Luxembourg, Luxembourg.*

Abstract

Spatially distributed riverbed bathymetry information are rarely available but mandatory for accurate hydrodynamic modeling. This study aims at evaluating the potential of the Global Navigation Satellite System (GNSS), like for instance Global Positioning System (GPS), for retrieving such data. Drifting buoys equipped with navigation systems such as GPS enable the quasi-continuous measurement of water surface elevation, from virtually any point in the world. The present study investigates the potential of assimilating GNSS-derived water surface elevation measurements into hydraulic models in order to retrieve effective riverbed bathymetry. First tests with a GPS dual-frequency receiver show that the root mean squared error (RMSE) on the elevation measurement equals 30 cm provided that a differential post processing is performed. Next, synthetic observations of a drifting buoy were generated assuming a 30 cm average error of water surface elevation (WSE) measurements. By assimilating the synthetic observation into a 1D-Hydrodynamic model, we show that the riverbed bathymetry can be retrieved with an accuracy of 36 cm. Moreover, the WSEs simulated by the hydrodynamic model using the retrieved bathymetry are in good agreement with the synthetic "truth", exhibiting an RMSE of 27 cm.

Keywords: Global Navigation Satellite System (GNSS) - Global Positioning System (GPS), Water Surface Elevation (WSE), effective bathymetry, hydrodynamic modeling, data assimilation

1. Introduction

The cost of damage caused by flooding is highly dependent on the warning time given before an event, making the issuing of timely flood alerts critical for minimizing the cost of flood damage. Predicting floods therefore remains a key concern of our society. Flood inundation models play a central role in real-time flood forecasting. In advanced hydro-meteorological forecasting systems, they provide information about expected flood hazard and damages. The models are used to accurately predict the timing and magnitude of a flood. The utility of any given model is, however, dependent on the availability of the necessary input data. Uncertainties in flood inundation modeling tend to be very high (Pappenberger et al., 2007), despite the physical laws that hydrodynamic models are generally based upon. This is partly a result of numerical approximations within hydrodynamic models, but it mainly derives from inadequate or lacking data on the geometry of the channel and the floodplain, the difficulty in estimating roughness coefficients and the uncertainty in initial and boundary conditions (Smith et al., 2009).

Channel and floodplain topography are required for setting up a hydrodynamic model. While the floodplain geometry can be extracted from freely available topography databases, it is important to mention that there is no database for the world's river bathymetries. The SRTM mission digital elevation model (DEM) for instance covers the Earth surface with a spatial resolution of 90 m. In addition, the Tandem-X mission DEM is expected to provide, from 2014 on, a global surface coverage with a spatial resolution of 12 m. However these data sources are known to have their inherent limitations, especially in narrow valleys and densely populated areas. More accurate elevation data sources like DEMs derived from airborne Lidar techniques can be an alternative for providing floodplain topography, but they come at a cost.

As a global database of river bathymetries does not exist, and because of the necessity to penetrate water

*Corresponding author, Email: hostache@lippmann.lu, Tel: +352 470261-417, Fax: +352 470264

for a direct measurement of bathymetry, time and cost intensive field campaigns are generally required.

In this context of lacking riverbed bathymetry data, Durand et al. (2008) and Yoon et al. (2012) showed that river Water Surface Elevation (WSE) measurements from the proposed Surface Water Ocean Topography (SWOT) satellite mission should be helpful for estimating bathymetries using assimilation techniques in hydrodynamic models. Based on a Ka-band SAR interferometer, SWOT will provide gridded WSE information for inland lakes and rivers wider than 50 m. The images provided by SWOT will have a 50 m spatial resolution on 120 km wide swath and the WSE is expected to be measured with a centimeter vertical accuracy over a 1 km^2 area (Alsdorf et al., 2007). In the previously mentioned proof-of-concept studies, synthetically generated SWOT observations of WSE were assimilated into the LISFLOOD-FP hydrodynamic model. Durand et al. (2008) were able to estimate bathymetry in five locations along the Amazon river with an accuracy of 56 cm using the ensemble Kalman filter. Yoon et al. (2012) made use of the local ensemble batch smoother (LEnBS) assimilation scheme and were able to estimate the bathymetry with a 52 cm reach average accuracy for the Ohio river after assimilating 8 virtual SWOT revisit cycles. SWOT is foreseen to be launched in 2020. This paper introduces an alternative technique, based on GNSS.

At present, only a limited number of research studies have investigated the potential of GNSS like GPS for WSE measurements. GNSSs are currently mostly used for monitoring sea level (Hong et al., 2008; Watson et al., 2008; Bisnath et al., 2003). Bisnath et al. (2003) found that real time kinematic (RTK) carrier phase is able to provide tide level estimates with a vertical accuracy of 10 cm. Moreover, Holtschlag and Aichele (2001) deployed drifting buoys equipped with GPS in order to investigate flow patterns and describe turbulent dispersion characteristics within river reaches. More recently in a case study on the river Mekong, Apel et al. (2012) showed that moored GNSS equipped buoys were able to provide WSE measurements with an accuracy of 2 cm.

In the light of these encouraging results and with the advent of advanced GNSS, such as Galileo, and with correction information (Differential GNSS) from networks of fixed stations becoming more readily available in near-real time, GNSS-supported measuring devices can be considered a promising alternative for obtaining WSE and flow velocities at a large number of locations.

Furthermore, over the last years, there has been a significant progress with respect to the integration of distributed hydrometric data with hydrodynamic models (e.g. Neal et al., 2007; Andreadis et al., 2007; Matgen et al., 2010; Hostache et al., 2010; Giustarini et al., 2011; Biancamaria et al., 2011).

In such data assimilation studies, modeled state variables or model parameters are sequentially verified and updated via measurements. The idea behind this is to merge the high temporal and spatial resolution of generally rather poor model predictions with more accurate but intermittent remote sensing observations to yield the best possible model simulations. Furthermore, if integrated with parameter estimation techniques, there is the potential to estimate uncertain model parameters, which may be used to increase the accuracy of the model (Montanari et al., 2009). Data assimilation techniques based on different versions of the Kalman filter have been used to assimilate ground gauge-based river level data at points along river reaches (Madsen and Skotner, 2005; Neal et al., 2007) from which discharge can be estimated through state augmentation. Despite this potential, applications of assimilation techniques with distributed stage data continue to be rare. In one of the few studies of this type, Andreadis et al. (2007) successfully used a square-root ensemble Kalman filter to assimilate synthetic WSE measurements from the proposed SWOT satellite mission with simulations from a hydrodynamic model for estimating river discharge. This study showed that the assimilation of 8 successive SWOT overpasses allowed a reduction of the relative error of discharge estimations from 23.2 % to 10 %. Lai and Monnier (2009) and Hostache et al. (2010) applied a variational data assimilation method using distributed WSE in order to combine in an optimal way measurement data and a 2D shallow water model. This assimilation process allowed (1) the identification of optimal Manning friction coefficients and (2) the identification of areas in the floodplain and the channel where frictions are homogeneous. Smith et al. (2009) assimilated distributed data from wireless sensor networks in a parsimonious time series model to produce forecasts with reduced uncertainty. Matgen et al. (2010), and later on Giustarini et al. (2011), demonstrated the usefulness of assimilating via a particle filter WSE derived from satellite SAR images to improve flood forecasts.

In this general framework, the study aims at proposing a synthetic experiment to evaluate the benefit of assimilating GNSS-derived WSE measurements into a hydrodynamic 1D model for effective bathymetry retrievals. It has to be noted here that we defined effective bathymetry in relation with a hydrodynamic model. Indeed we defined in this study the effective bathymetry as the river channel geometry allowing for correctly pre-

dicting flood propagation using a given model. As a matter of fact, an effective bathymetry is defined in relation to a given hydrodynamic model with given parameters and simplifications, but the methodology presented is this paper remains generic and can be applied using other hydrodynamic models. Moreover, during this study we made use only of GPS, but the same method can be applied to any other kind of GNSS.

2. Material and methods

This section introduces the design of a GPS buoy and proposes an assimilation technique for effective bathymetry retrievals. Moreover, it describes a synthetic experiment allowing to assess the usefulness of assimilating WSE provided by the buoy into a hydraulic model. In the context of a proof-of-concept study, the main advantage of using synthetically generated data rather than actual measurements is to allow for controlling the errors and their structure. It is important and necessary to demonstrate the efficiency of an assimilation scheme in a controlled environment before it can be applied to actual measurements. Moreover, a synthetic experiment, with known errors, facilitates the identification of advantages and drawbacks of the procedure itself.

2.1. Designing the GPS Buoy

The aim of the GPS-equipped buoy is to provide WSE measurements with sufficient accuracy, in order to enable the retrieval of riverbed bathymetry through data assimilation. Based on the evaluations of Hostache et al. (2009) and more recently Matgen et al. (2010), we define an elevation measurement accuracy of 30 cm as a target value for GPS-derived WSE measurements. The system is composed of a water-proof canoe-box with a transparent hemispheric lid, filled with an integrated dual-frequency GPS, namely the Hemisphere A221^{TM} Smart Antenna. The hemispheric lid is used to limit potential GPS signal perturbations. To protect it from strong shocks during deployment and to ensure its buoyancy and stability, the integrated system is surrounded by a tire (Figure 1). The two frequencies, L1/L2, of the GPS receiver allow correcting the major part of the positioning errors due to the ionosphere (Kim and Tinin, 2009). In addition, a Post Processing Kinematic treatment is applied to the data in order to reduce bias and noise. For this post treatment we take advantage of the Luxembourg network of permanent GNSS stations (SPSLux). These reference stations, with accurately known coordinates and altitudes, enable the estimation of the correction parameters. The latter can be used to correct the error associated with a rover GPS receiver in differential mode, provided that the rover is not too distant from the reference station (Apel et al., 2012). In case a reference GPS station would not be available, an alternative would be to make use of OMNISTAR (Martinez et al., 2000), that offers a worldwide differential GPS service, based on reference stations, high power satellites and global network control centers (`www.omnistar.com`).

It is worth mentioning that a hydro-acoustic sensor, such as a sonar or Acoustic Doppler Current Profiler (ADCP) mounted on a buoy, can be considered as an alternative for obtaining riverbed bathymetry. These systems provide a means for directly measuring water depth. However, in this study we adopted an indirect retrieval technique based on GPS data that is less sensitive to the stability of the buoy and that is not impacted by the sediment concentration in the water (due to bedload in particular). These two aspects are known to significantly increase the measurement errors associated with hydro-acoustic sensors.

2.2. Assimilating GPS derived water surface elevation

This section presents the general framework of the assimilation scheme. More specific details related to the hydrodynamic model and the synthetic experiment are presented in section 2.3.

The aim of the assimilation technique is to exploit WSE recorded by a GPS in order to retrieve unknown bathymetry.

The data assimilation scheme applied in this study is a modified version of the Particle Filter (PF). The particle filter is an ensemble-based assimilation technique. This means that the prior probability of a state variable is estimated using a sample of model simulations (Smith et al., 2008). The PF computes posterior probabilities of state variables using a weighting procedure. In the PF, there is no need to formulate restrictive hypotheses on the model and observation density functions (Moradkhani, 2007). This is a key advantage of the PF with respect to the more widely used Ensemble Kalman Filter EnKF (e.g. Burgers et al., 1998; Evensen, 1994).

In this study, we use a variant of a PF that we propose to call particle smoother (PS) hereafter. This variant of the PF is comparable to the one proposed by Dunne and Entekhabi (2005) for the ensemble Kalman filter. This means that all observations distributed over time are assimilated at once to update the model state variables at any time step. According to Plaza et al.

(a) (b)

Figure 1: Photograph of the GPS buoy (a) outside the water and (b) drifting in the Alzette river stream.

(2012) this kind of smoother can be compared to variational assimilation techniques.

The implementation used in this study is based on the Sequential Importance Sampling (SIS) method. In our study, each particle consists of a possible state of the variables, namely the WSE simulated over time and space using one hydrodynamic model. Each hydrodynamic model is based on one realization of the bathymetry. In other words, one particle correspond to the WSE (distributed over space and time) simulated by one hydrodynamic model using one bathymetry realization. Section 2.3 explains how the ensemble of bathymetry realization is generated. The number of state variables for a given particle corresponds to the number of elements in the geometry of the model domain multiplied by the number of time steps. In this study, we make use of a one-dimensional hydrodynamic model (see section 2.3.1). In such a model, the geometry is defined by cross sections perpendicular to the main flow direction. For simplifying the riverbed representation and facilitating the data assimilation process, it is assumed here that the targeted riverbed bathymetry is of rectangular shape (see Figure 2) with a known river width (RW). The riverbed is thus characterized by only one parameter, the river depth (RD). Of course, real riverbeds are rarely of rectangular shape. However, we believe that this simplification is sensible for this study as it allows validating the new concept and, in the same time, does not prevent the model from generating realistic results. It is also worth mentioning that the same assumption has been made in similar proof-of-concept studies (e.g. Durand et al., 2008; Yoon et al., 2012). Finally, the method introduced in this study can be extended to more complex geometries.

In a PF, the filtering density is approximated by a discrete distribution, whose support is the set of particles. The probability mass assigned to each particle is proportional to that particle's weight, which, in turn, is proportional to the likelihood of the observation at the assimilation time step (Fearnhead, 2002). The particles are sampled directly from the state-space to represent the posterior probability, and a local weight is computed for each particle at each cross section and at each time step, according to the information contained in the observations: a local weight, $w^{i,j,k}$, is assigned to an observed cross section j for a particle i, at an observation time step k. Note that the weighting procedure can be adapted to any kind of distribution function. When assimilating data stemming from the GPS buoy, a Gaussian likelihood was used, assuming the mean of recorded WSE to represent the mean of a normal distribution whose shape is defined by a pre-defined value of standard deviation. A local weight, $w^{i,j,k}$, is therefore computed for a WSE $x^{i,j,k}$ simulated by particle i at cross section j and time step k, for which an observation is available:

$$w^{i,j,k} = \frac{1}{\sigma\sqrt{2\pi}} e^{\frac{-\left(x^{i,j,k}-\mu^{i,j}\right)^2}{2\left(\sigma^{i,j}\right)^2}} \quad (1)$$

In Eq. 1, x is the matrix of the state variables (WSE at cross section j and time step k simulated by particle i), μ is the observation mean and σ is the standard deviation associated with the observations. The matrix of weights contains all local weights, $w^{i,j,k}$. Subsequently, one global likelihood is computed for each particle and each cross section by applying the joint probability the-

ory for independent variables:

$$\omega^{i,j} = \prod_{k=1}^{N_o} w^{i,j,k} \quad (2)$$

where N_o is the number of observation time steps. The resulting global weights are then normalized using Eq. 3.

$$W^{i,j} = \frac{\omega^{i,j}}{\sum_{i=1}^{N_p} \omega^{i,j}} \quad (3)$$

In Eq. 3, N_p is the number of particles. Next, the global weights allow for the computation of an expectation of the updated WSE:

$$E(x^{i,j,k}) = x_{exp}^{j,k} = \sum_{i=1}^{N_p} W^{i,j} x^{i,j,k} \quad (4)$$

To update the riverbed bathymetry, we propose to correct each river bathymetry realization by shifting the corresponding riverbed bottom elevation using a distance equal to the time-averaged deviation between the WSE simulated by this particle and the expected WSE:

$$UpBOE_{i,j} = BOE_{i,j} + \sum_{k=1}^{N_o} \frac{x^{i,j,k} - x_{exp}^{j,k}}{N_o} \quad (5)$$

In Eq. 5 $BOE_{i,j}$ and $UpBOE_{i,j}$ represent respectively the first guess and the updated bathymetry (for particle i at model cross section j) as shown in Figure 2. It is worth noting that each cross section bathymetry is updated with an independent $\delta^{i,j} = \sum_{k=1}^{N_o} \frac{x^{i,j,k} - x_{exp}^{j,k}}{N_o}$.

Subsequently, new model simulations are performed using the updated bathymetry realizations, before a new assimilation process is carried out. This bathymetry update cycle is then repeated until a convergence of bathymetry realizations is obtained (i.e. until a predefined tolerance criterion is satisfied).

Figure 2 presents the flowchart of the assimilation scheme.

2.3. Designing the synthetic experiment

In this part of the paper we propose a synthetic experiment in order to evaluate the value of GPS-derived WSE measurements for retrieving riverbed bathymetry. This experiment makes use of a calibrated hydrodynamic model. The next paragraph (see 2.3.1) introduces this model and its calibration. Paragraph 2.3.2 explains how the synthetic observations have been generated using this model. Finally, paragraph 2.3.3 proposes a method for generating the ensemble of model simulations.

2.3.1. The hydrodynamic model

The set up and calibration of the hydrodynamic model is described in Hostache et al. (2009). This model has been developed using the freely available Hec-RAS software (USACE, 2002). Hec-RAS performs unsteady simulations by solving the 1Dimensional de Saint-Venant equation using an implicit finite difference approximation. Hostache et al. (2009) calibrated two Manning friction coefficients: one for the river channel (n_c=.047) and one for the floodplain (n_{flp}=.182). During the calibration process, Monte-Carlo simulations within ranges of plausible Manning parameters were carried out. The upstream boundary condition was the observed discharge hydrograph. The parameter set providing the best performance with respect to both observed downstream discharge hydrographs and remote sensing-derived WSE distributed across the floodplain was selected as optimal (see Hostache et al., 2009, for more details). It has to be noted here that in spite of the necessity to carry out the experiment in a realistic set up, the calibration of the hydrodynamic model is not the main issue of the study. Indeed, the objective is to retrieve an effective bathymetry that allows the model to yield correct predictions of flood wave propagation in terms of discharge and water surface elevation. Therefore, slightly different values of friction would most likely result in slightly different values of the retrieved effective bathymetry.

2.3.2. The synthetic observations

The method that was adopted for generating synthetic observations aims at creating a synthetic dataset that is representative of a dataset that could be obtained from the GPS buoy. To do so, we propose a two-step approach, namely (i) to generate a so-called synthetic truth by a forward run of the calibrated hydrodynamic model, (ii) to perturb the so-called truth in order to generate synthetic observations with controlled errors.

In the experiment, we assume that for several days a buoy is launched at the upstream end of the river reach. This is done every day at the same time. The buoy is left drifting freely in the river and is then recovered when it reaches the downstream end. This means that many free drifting cycles (one per day) of measurements are obtained from such an experiment.

The one-dimensional hydrodynamic model (see 2.3.1) provides as output the cross section-averaged flow velocity and the WSE at each cross section of the model for every time step of the simulation. We obtained the synthetic truth from a forward run of the calibrated hydraulic model. In our scenario, a buoy is

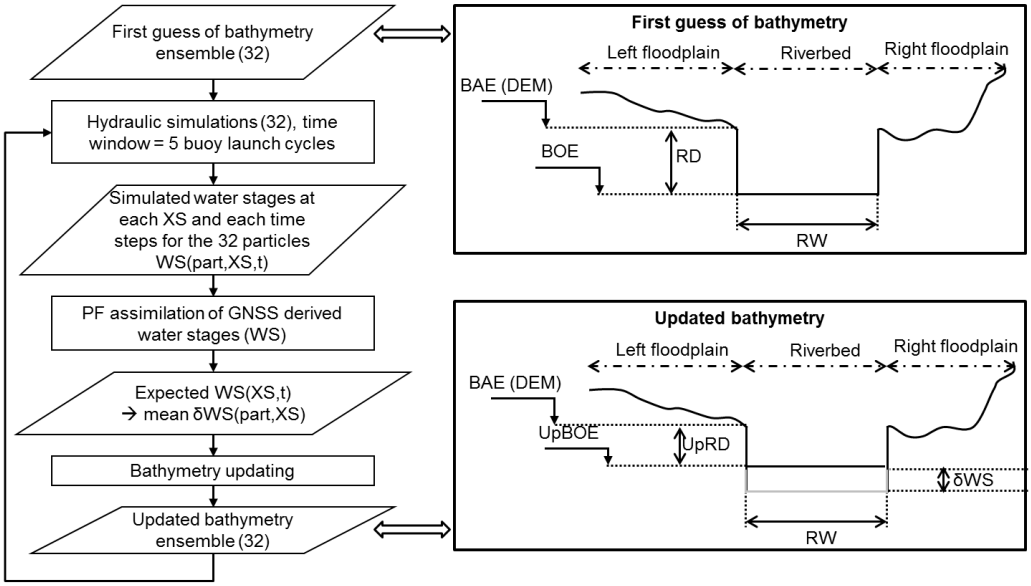

Figure 2: Flowchart of the assimilation method.

launched at the upstream boundary of the river. Assuming that the buoy velocity equals the cross section-averaged flow velocity provided by the model, it is possible to predict the buoy position at every step, by sequentially multiplying the velocity value by the time step duration. By repeating this computation for each time step, it is then possible to estimate the position of the synthetic buoy. As the model also provides WSE, the synthetic truth consists of the buoy location, namely the model cross section on which it is located, and the corresponding simulated WSE.

Finally, synthetic WSE observations are derived by adding to the synthetic truth a normally distributed noise, whose mean and standard deviation are set to values that are representative of the data that are expected to be obtained using the actual GPS. It is worth noting that, at each time step, only one value of WSE at a given position is provided by the synthetic GPS buoy.

2.3.3. The particle ensemble set up

Our experiment consists of assimilating synthetic WSE observations into an ensemble of hydraulic models, whose upstream boundary condition is a flow hydrograph obtained by the means of continuous *in situ* WSE measurements and a rating curve.

The truth and the ensemble of model predictions were generated separately: they share the same model structure, parameters, forcings and initial conditions, however the geometry components differ. In fact, to create the so-called truth, a hydraulic model run has been performed using the observed geometry composed of a floodplain Lidar DEM and a ground surveyed riverbed bathymetry (see section 2.3.2). For the bathymetry retrieval exercise, on the other hand, we removed the bathymetry information and we assumed the riverbed to be of rectangular shape (see Figure 2). To create the ensemble of model predictions, we randomly generate 32 possible realizations, representing a first guess of the bathymetry. To do so, the unknown riverbed shape is assumed to be of rectangular type, with a given river depth (RD) and a given river width (RW) (see Figure 2). It is assumed here that the bank elevation (BAE, see Figure 2) and the floodplain geometry are determined using an available digital elevation model (e.g. the globally available SRTM DEM with a spatial resolution of 90 m). We also suppose that the river width RW can be obtained from optical satellite data or any other source of information. According to these two assumptions, the river bathymetry is defined by the river depth RD (Figure 2), with the river bottom elevation BOE being obtained by subtracting RD from BAE.

For each cross section of the hydrodynamic model, random values of RD are generated in order to obtain a first guess of the bathymetry. To maintain a certain hydraulic consistency of the randomly generated river depth of each particle, we suggest the following two-step approach:

1. random generation of 32 plausible values of RD (one for each particles), that are subtracted from BAE values along the river reach to obtain the bed level for each particle,
2. random perturbation at the cross section level (error with uniform distribution centered on 0 and with a range equal to 25 % of the randomly generated RD value for the specific particle).

This two-step approach ensures a good computational stability of the hydrodynamic model, as non-plausible RD values could lead to more time-consuming and failing computations. It has to be noted here that we expect the number of bathymetry realizations not to be of major importance. The number of realizations does have some influence on the time it takes for the assimilation algorithm to converge. However, our experiments show that the final bathymetry estimate is not significantly affected by the number of particles. As a matter of fact, the number of realizations has been set to 32 as this number was considered a good compromise between computational efficiency and convergence capability. In our opinion, the key point for efficiently retrieving the bathymetry is to ensure that the spread of the realizations encompasses all the values that could *a priori* be expected for the real bathymetry. To evaluate the generated ensemble, we computed two verification measures proposed by De Lannoy et al. (2006), namely the ratio between the averaged ensemble skill and the averaged ensemble spread (called VM_1 hereafter) and the ratio between the average squared ensemble skill and the averaged root mean squared error computed between simulation and observation (called VM_2 hereafter). According to De Lannoy et al. (2006), VM_1 might be close to one to guaranty that the ensemble spread is of the order of magnitude of the model deviation to observation. A value of VM_1 higher than 1 means that the ensemble spread is too small whereas a value of VM_1 lower than one means that the ensemble spread could be further reduced. According to De Lannoy et al. (2006), with 32 particles, VM_2 might be equal to 0.72 for the observation and the ensemble to be statistically undistinguishable.

At this stage of the methodology, a first guess of the geometry has been defined via a set of 32 realizations of the river bathymetry. Each particle corresponds to a hydrodynamic model making use of one bathymetry realization. It is worth mentioning that for a given particle, the RD value is different at each cross-section. After the first guess of the bathymetry has been generated, the assimilation algorithm as defined in section 2.2 is applied.

3. Study area and available data

The area of interest is located in the Grand Duchy of Luxembourg (see Figure 3).

The basin area is about 356 km^2 at the stream gauge located in Pfaffenthal where WSE is recorded every 15 min. The corresponding discharge hydrograph has been estimated using the rating curve of this hydrometric station. It constitutes the upstream boundary condition of the hydrodynamic model, which simulates the 19 km reach of the Alzette River between the hydrometric stations at Pfaffenthal and Mersch (Hostache et al., 2009). The river reach is described by 158 ground-surveyed channel cross sections whereas the floodplain topography has been extracted from a Lidar DEM of 2 m pixel spacing and 15 cm vertical accuracy (see Hostache et al., 2009, for more details). Moreover, aerial photographs with 50 cm spatial resolution were available for the area of interest and used to determine river width.

The synthetic experiment is grounded on a real storm event starting on January 2 2012 and ending on January 6 2012. During these five days there were high variations of discharge without overbank flooding. These characteristics of the event are rather important, as they imply that the buoy would have kept drifting inside the riverbed during the experiment and would have provided WSE observations associated with different flow conditions.

4. Results and discussion

This section first presents and discusses the results of "dry" tests (i.e.: carried out outside the water) of the GPS buoy. Next it focuses on the data assimilation experiment and discusses its outcome.

4.1. Evaluating the vertical accuracy of the GPS buoy

The "dry" tests that have been carried out provide some insights into the accuracy levels that can be achieved when deploying the buoy inside a river. The road and the parking lot around the research institute (Belvaux, Luxembourg) offer an appropriate test site for the system. With the "canyon" of surrounding buildings and their impact on the GPS signal, the study site shares some similarities with a river channel where double bounce effects caused by trees and the river banks cause also perturbations. Moreover, a loss of signal is possible due to the surrounding trees, banks or buildings, that also mask out part of the sky, thereby reducing the number of available GPS satellites. For this study site, the

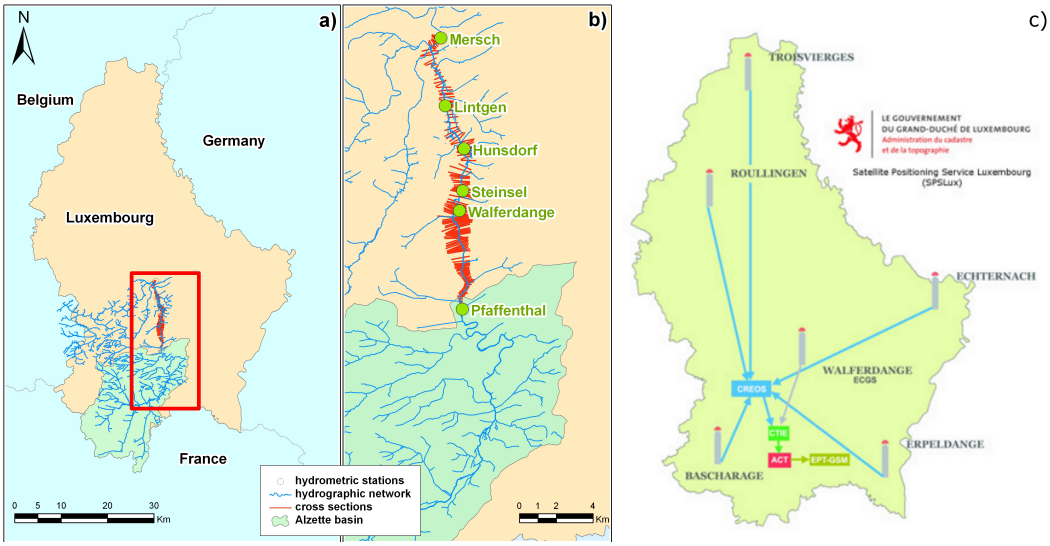

Figure 3: Study site in the Alzette River basin showing: (a) the drainage area down to Pfaffenthal and the 19 km river reach whose geometry is represented by the cross sections, (b) the hydrometric stations along the river, c) the SPSLux refence GPS station map (source http://www.act.public.lu).

closest SPSLUX reference station is located in Baschar-age at a distance of 16 km (see Figure 3c).

To carry out the experiment in "dry" conditions, the first step was to define a set of reference points with accurately-known geographic coordinates and altitudes. To do so, a theodolite was used, enabling the positioning with an associated planimetric and altimetric accuracy of less than 1 cm. 60 reference points have been marked on the ground and accurately located on the site. Next, by moving the GPS buoy along the pre-defined path and using a stopwatch as time recorder, it was possible to estimate the accuracy of the positioning. Each time the GPS receiver passed over a mark on the ground, the relative time from the beginning of the test was recorded using the stopwatch. This relative time was converted into absolute time using the GPS time at the beginning of each test. The known position of the marks was then compared with the position measured by the GPS at the time recorded by the stopwatch.

The results of this test showed that the elevation information provided by the system may be biased if specific time steps are considered. However, over four test campaigns spread over two days and at various daytimes, it appeared that the mean altimetric error equaled 0 cm and its standard deviation 30 cm. Figure 4 presents the GPS altimetric measurement errors recorded during the experiment. These values were used as a basis for defining the observational errors in the synthetic experiment.

It is worth mentioning here that other GNSS could be used in addition to GPS, like for instance Glonass and the upcoming Galileo, in order to increase the GNSS measurement accuracy and to avoid signal losses especially when the number of visible satellites becomes critically low.

4.2. Generating synthetic observation

To create synthetic observations we followed the procedure presented in paragraph 2.3.2. To do so, we performed a forward run of the calibrated hydraulic model using the measured geometry data. The upstream boundary condition used for this model run was the discharge hydrograph recorded by the Pfaffenthal stream gauge. During this model run (between January 2 and 6 2012), with a simulation time step of one minute, the simulated WSE and the cross-section-averaged flow velocities at all the cross sections have been stored. Assuming that a buoy is launched every day at 7:00 AM and drifts freely at the cross-section-averaged flow velocity, the results of the hydrodynamic simulation allow calculating the position of the buoy and the corresponding WSE at each time step (see section 2.3.2). The position and the elevation of the buoy represent the so-called "truth". Next, the "truth" has been perturbed using a normally distributed noise with a mean of 0 m and a standard deviation of 30 cm.

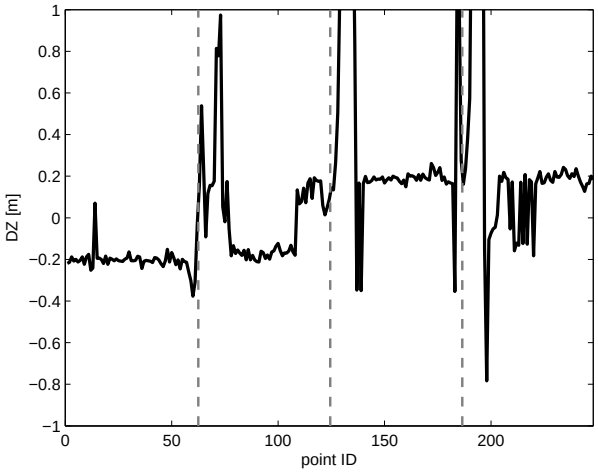

Figure 4: Summary of measurement error during the GPS dry condition test. The black line represent the measurement error whereas the gray dotted vertical lines identify the four field campaigns.

4.3. Retrieving bathymetry via assimilation of synthetic observations

The aim of the synthetic experiment is to evaluate the potential added value of WSE measurements provided by the developed GPS buoy for bathymetry retrievals. As introduced in section 2.2, the assimilation procedure is carried out iteratively using the full set of WSE observations.

As proposed in paragraph 2.3.3, to create the ensemble of model predictions 32 realizations of the bathymetry were generated. Bank elevation (BAE, see Figure 2) and floodplain geometry were extracted for each cross-section from the available Lidar DEM. The river widths RW were determined by digitizing the river banks using the aerial photographs (see section 3). The river bathymetry is then created by randomly generating RD values following the two-step approach proposed in section 2.2:

1. 32 plausible values of RD were drawn from a uniform distribution ranging between 0 and 20 m (one for each particle) and subtracted from the BAE value along the river reach to obtain the bed level for each particle,
2. a random noise was added to each cross-section riverbed (error with uniform distribution centered on 0 and with a range equal to 25 % of the randomly generated RD value for the specific particle).

The first guess of the bathymetry is presented in Figure 5a. In this figure, each light gray line corresponds to one particle of the ensemble, whereas the bold black and grey lines represent the observed bathymetry and the ensemble mean, respectively. It is worth specifying that what we call observed bathymetry is actually not the lowest point of the riverbed extracted from the ground surveyed cross sections. Instead, considering that the ground-surveyed channel cross sections do not have a rectangular shape, we computed an equivalent rectangle-shaped bathymetry, having hydraulic properties equivalent those of the observed one. In other words, from each real cross-section we computed the "observed" RD so that the corresponding rectangle-shaped cross-section has, under the assumption of steady flow conditions, a rating curve (discharge/WSE relationship) as close as possible to that of the true riverbed cross-section. This computation has been carried out iteratively, based on the optimization of the Manning-Strickler formula. As a matter of fact, the so-called observed bathymetry corresponds to the rectangular-shaped equivalent of the true bathymetry.

As proposed in section 2.3.3, to evaluate the generated ensemble, we computed two verification measures proposed by De Lannoy et al. (2006). In our study, computed on WSE, VM_1 is equal to 0.62 which means that the ensemble spread could be further reduced but can however be correctly used. Furthermore, VM_2 is equal to 0.61, which means that the ensemble and the observation are statically distinguishable, but similar. As a matter of fact, the two verification measures indicate that the 32 generated particles can be used correctly in an assimilation framework.

Figure 5b, c and d show, respectively, the results of the assimilation after iterations 1, 3 and 10. In Figure 5a, it is worth noting that the spread of the ensemble first guess is rather large and that the ensemble mean is distant from the bathymetry observation. After the first iteration, Figure 5b shows that the spread of the particles is significantly reduced. After three iterations, the spread of the particles is more reduced (Figure 5c) and, after ten iterations (Figure 5d), the ensemble fully converges, i.e. all the particles overlap. In addition, Figure 6 presents the water surface elevation lines (along the river reach) simulated by the model at a time step close to the flood peak, for various assimilation iterations. This figure demonstrates that the simulated water levels quickly converge toward the so-called synthetic truth.

Figure 7 shows two performance criteria of the updated bathymetry and one performance criterion of the simulated WSE computed after each iteration of the assimilation algorithm. In Figure 7, the black line represents the spread of the bathymetry ensemble. This line shows that the spread is almost reduced to zero after 8 iterations. In the same figure, the light and middle grey lines correspond respectively to the root mean squared error (RMSE) and the mean error (ME) between the average of the bathymetry ensemble and the observed bathymetry. When analyzing the behaviour of the ensemble spread, the RMSE and the ME are quite similar, in the sense that they reach a plateau after several iterations. The lowest RMSE that is reached after several iterations equals 36 cm, whereas the lowest obtained ME is close to 0 cm. These results are encouraging, as they demonstrate that the observed and the retrieved bathymetries are in good agreement. An iterative repetition of the assimilation technique allows for an efficient retrieval of the bathymetry.

When having a closer look at Figure 5d, one can notice that the general trend of the observed bathymetry is well reproduced, despite the local topography not being described in all details. This indicates that the method enables the computation of the main characteristics of the bathymetry, but has its limitations for describing bathymetry changes at small scale. The retrieved bathymetry indeed appears as a smoothened estimate of the true bathymetry. To understand the origin of this effect, it is important to consider how the bathymetry influences WSE. Only bathymetry features having a significant effect on the WSE have a chance of being retrieved using the method. It can be argued that some of the small scale bathymetry features only have a limited effect on the WSE. Consequently, given the WSE measurement uncertainty (30 cm in this study), these features are not detectable with the proposed method.

In addition, Figure 7 shows the RMSE calculated between the mean of the simulated WSE ensemble and the truth. It is worth noting that after four iterations, the RMSE computed on WSE reaches a plateau at a value equalling 27 cm. This result is also encouraging as it shows that the WSE is correctly simulated despite the small scale bathymetry not being retrieved in all its details. Furthermore, this shows that the hypothesis of a rectangular shaped riverbed is acceptable as in spite of this simplification the model reaches a satisfying level of accuracy in terms of simulated water levels. Moreover, this 27 cm value must be mirrored with the error of 30 cm imposed to the synthetic GPS measurements. This demonstrates the reliability of the assimilation technique as the error of the simulated WSE is lower than the error of the synthetic observations.

5. Conclusions

The study presented in this paper focused on the potential benefits deriving from assimilating WSE observations provided by a drifting GNSS-equipped buoy into a hydrodynamic model for effective bathymetry retrievals.

A GPS buoy has been designed for measuring WSE. To reach a satisfactory accuracy level of WSE measurements, this buoy includes an integrated dual-frequency GPS, namely the Hemisphere A221^{TM} Smart Antenna, used in differential mode. By testing this GPS in "dry" conditions we were able to estimate an elevation measurement accuracy of 30 cm. For the assimilation exercise, in order to keep control on the model and measurement errors we carried out synthetic experiments. This allowed us to analyze, in a controlled environment, the added-value the GNSS-derived data sets may provide to hydraulic modeling and bathymetry retrievals. In this paper, we only made use of GPS, but it is worth noting that the extension to other GNSS, such as the upcoming Galileo, is feasible and may improve the GPS measurement accuracy.

The assimilation algorithm that was used is based on the Particle Filter, following the work of Giustarini et al. (2011). The proposed variant of the PF, termed in this paper particle smoother, is based on a global weighting procedure: a single particle contains, as state matrix, WSE at all cross sections and all time steps. The likelihood of each particle is derived from its ability to correctly predict WSE at the buoy's locations. Next, these likelihoods are used to estimate an expectation of the

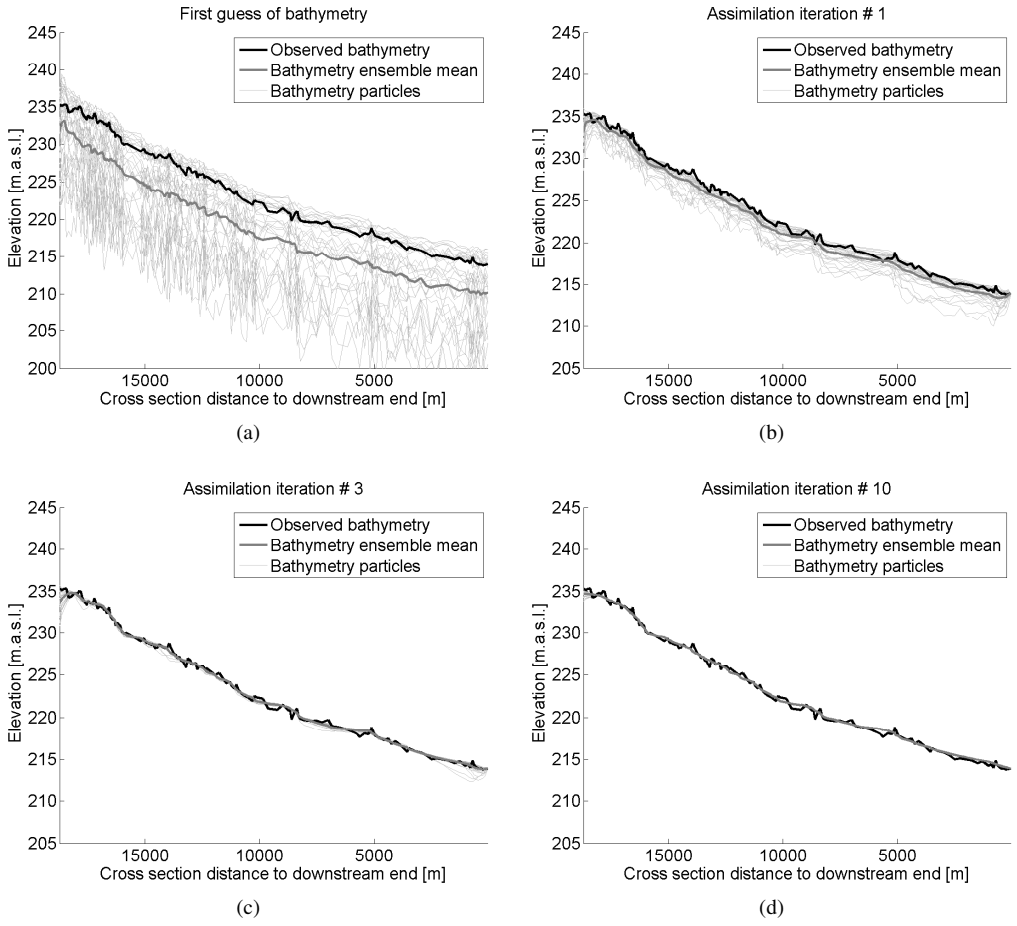

Figure 5: Bathymetry retrievals: first guess (a), and updated bathymetry after assimilation iterations 1 (b), 3 (c) and 10 (d).

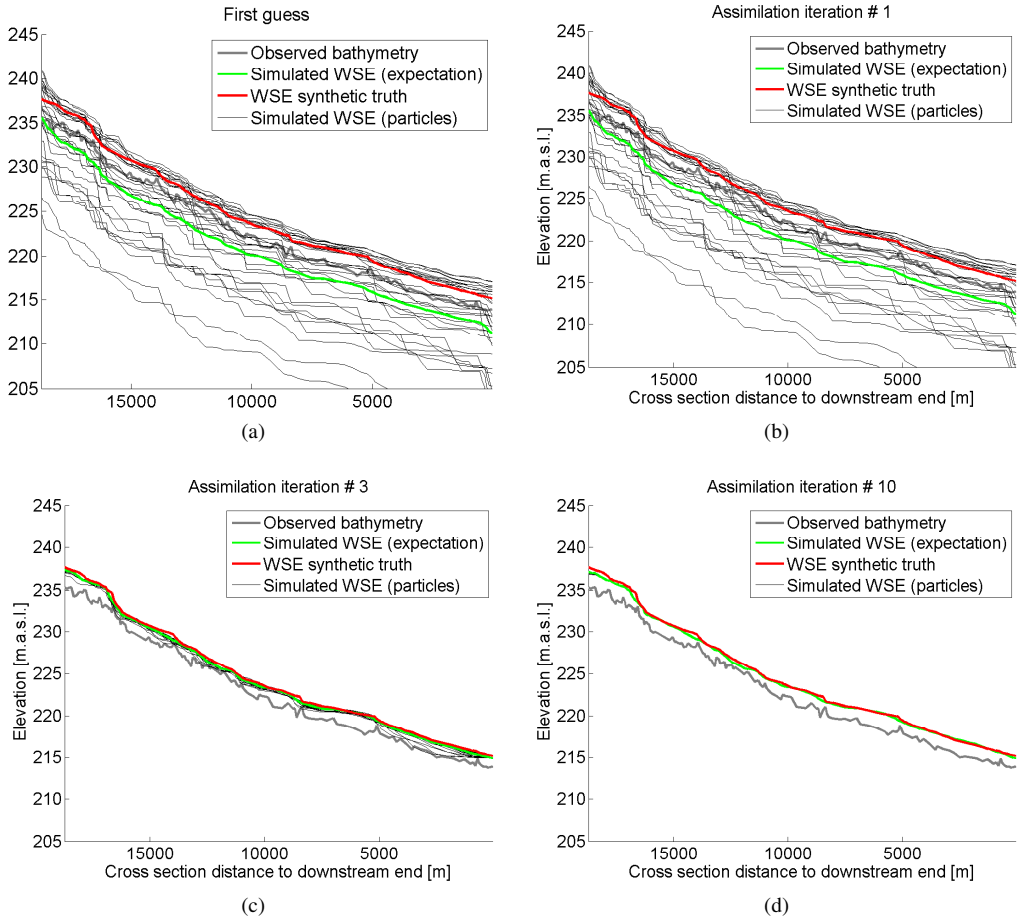

Figure 6: Simulated water surface elevation profiles (close to flood peak) after various assimilation iteration : open loop (a), and after assimilation iterations 1 (b), 3 (c) and 10 (d).

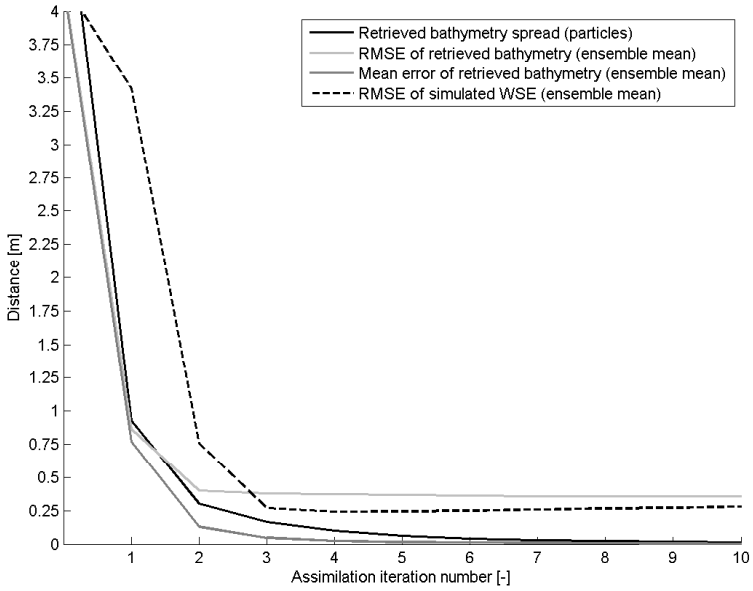

Figure 7: Bathymetry retrieval performance

WSE, that is later used to update the rectangular-shaped bathymetry associated with each particle.

In the assimilation scenario proposed in this study, one buoy is launched once a day during five subsequent days, implying that at a given time a single buoy is drifting along the channel. The assimilation is performed iteratively, in order to get gradually closer to the true bathymetry. The results show that the method enables the retrieval of the bathymetry with an accuracy of 36 cm. This result is promising and slightly better than the 56 cm and 52 cm obtained in similar studies by Durand et al. (2008) and Yoon et al. (2012). The general trend of the observed bathymetry is well reproduced while some of the small scale bathymetry features were missed out. The simulated WSEs are also in good agreement with the synthetic truth as the computed root mean squared error is equal to 27 cm.

The next step will be to carry out similar experiments with actual measurements. One further development of the assimilation and updating technique will be to analyze the added value of considering more realistic cross-section shapes, like a trapezoidal shaped cross-section. Moreover, one key issue of such techniques will be the retrieval of Manning friction coefficients in addition to bathymetry, as already proposed by Durand et al. (2008).

6. Acknowledgements

This study was part of the FLOODTRACKER project, financed by the National Research Fund (FNR) of the Grand Duchy of Luxembourg in the framework of the CORE research program (Contract no. C09/SR/19). Giovanni Corato's contribution was supported by the National Research Fund of Luxembourg through the FLOODMOIST project (SR/02/152).

We would like to thank several people with whom we discussed these ideas over the past years. We would like to mention in particular Laurent Pfister (with CRP-Gabriel Lippmann). We would like also to thank several people for sharing their expertise in GNSS with us, in particular Willy Croi, Arnaud Vacelet, Joan Fort (Luxspace S.A.), Tonie van Dam (University of Luxembourg) and Bernard Reisch (Administration du Cadastre et de la Topographie, Luxembourg).

References

Alsdorf, D., Rodriguez, E., Lettenmaier, D., 2007. Measuring surface water from space. Rev. Geophys. 45.

Andreadis, K. M., Clark, E. A., Lettenmaier, D. P., Alsdorf, D. E., 2007. Prospects for river discharge and depth estimation through assimilation of swath-altimetry into a raster-based hydrodynamics model. Geophys. Res. Lett. 34, 5.

Apel, H., Hung, N., Thoss, H., Schne, T., 2012. Gps buoys for stage monitoring of large rivers. J. Hydrol. 412-413, 182–192.

Biancamaria, S., Durand, M., Andreadis, K., Bates, P., Boone, A., Mognard, N., Rodriguez, E., Alsdorf, D., Lettenmaier, D., Clark,

E., 2011. Assimilation of virtual wide swath altimetry to improve Arctic river modeling. Remote Sens. Environ. 115, 373–381.

Bisnath, S., Wells, D., Howden, S., Dodd, D., Wiesenburg, D., 2003. Development of an operational RTK GPS-equipped buoy for water level recovery. In: Proceedings of ION GPS/GNSS 2003. Portland, OR, 9-12 September 2003.

Burgers, G., Leeuwen, P. J. V., Evensen, G., 1998. Analysis scheme in the ensemble Kalman filter. Mon. Weather Rev. 126, 1719–1724.

De Lannoy, G. J. M., Houser, P. R., Pauwels, V. R. N., , Verhoest, N. E. C., 2006. Assessment of model uncertainty for soil moisture through ensemble verification. J. Geophys. Res. 111 (D10101).

Dunne, S., Entekhabi, D., 2005. An ensemble-based reanalysis approach to land data assimilation. Water Resour. Res. 41.

Durand, M., Andreadis, K. M., Alsdorf, D. E., Lettenmaier, D. P., Moller, D., Wilson, M., 2008. Estimation of bathymetric depth and slope from data assimilation of swath altimetry into a hydrodynamic model. Geophys. Res. Lett. 35 (20), L20401.

Evensen, G., 1994. Sequential data assimilation with a nonlinear quasigeostrophic model using Monte Carlo methods to forecast error statistics. J. Geophys. Res. 99 (C5), 10143–10162.

Fearnhead, P., 2002. Markov chain Monte Carlo, sufficient statistics, and particle filters. J.Comput. Graph. Stat. 11, 848–862.

Giustarini, L., Matgen, P., Hostache, R., Montanari, M., Plaza, D., Pauwels, V. R. N., De Lannoy, G. J. M., De Keyser, R., Pfister, L. Hoffmann, L., Savenije, H. H. G., 2011. Assimilating SAR-derived water level data into a hydraulic model: a case study. Hydrol. Earth Syst. Sci. 15, 2349–2365.

Holtschlag, D. J., Aichele, S., 2001. Visualization of drifting buoy deployments on St. Cr River near public water intakes. Tech. rep., U.S. Geological Survey Open File Report 01-17.

Hong, J., Backa, K., Park, U., Lee, D., Cha, S., 2008. Determination of ocean datum using GPS buoy observation data. In: The International Archives of the Photogrammetry, Remote Sensing and Spatial Information Sciences. Vol. XXXVII. Part B8. Beijing, China, pp. 685–688.

Hostache, R., Lai, X., Monnier, J., Puech, C., 2010. Assimilation of spatially distributed water levels into a shallow-water flood model. Part II: Use of a remote sensing image of Mosel River. J Hydrol 390 (3-4), 257–268.

Hostache, R., Matgen, P., Schumann, G., Puech, C., Hoffmann, L., Pfister, L., 2009. Water level estimation and reduction of hydraulic model calibration uncertainties using satellite SAR images of floods. IEEE T. Geosci. Remote 47 (2), 431–441.

Kim, B., Tinin, M., 2009. The association of the residual error of dual-frequency global navigation satellite systems with ionospheric turbulence parameters. J. Atmos. Sol. Terr. Phys. 71 (17-18), 1967–1973.

Lai, X., Monnier, J., 2009. Assimilation of spatially distributed water levels into a shallow-water flood model. Part I: Mathematical method and test case. J Hydrol 377 (1–2), 1 – 11.

Madsen, H., Skotner, C., 2005. Adaptive state updating in real-time river flow forecasting - a combined filtering and error forecasting procedure. J. Hydrol. 308, 302–312.

Martinez, J., Martinez, M., Garcia-Cerezo, A., 2000. A new method of generating differential GPS corrections. Control Eng. Pract. 8 (3), 253 – 258.

Matgen, P., Montanari, M., Hostache, R., Pfister, L., Hoffmann, L., Plaza, D., Pauwels, V. R. N., De Lannoy, G. J. M., De Keyser, R., Savenije, H. H. G., 2010. Towards the sequential assimilation of SAR-derived water stages into hydraulic models using the particle filter: proof of concept. Hydrol. Earth Syst. Sci. 14, 1773–1785.

Montanari, M., Hostache, R., Matgen, P., Schumann, G., Pfister, L., Hoffmann, L., 2009. Calibration and sequential updating of a coupled hydrologic-hydraulic model using remote sensing-derived water stages. Hydrol. Earth Syst. Sci. 13, 367–380.

Moradkhani, H., 2007. Hydrologic remote sensing and land surface data assimilation. Sensors 8, 2986–3004.

Neal, J. C., Atkinson, P. M., Hutton, C. W., 2007. Flood inundation model updating using an ensemble kalman filter and spatially distributed measurements. J. Hydrol. 336, 401–415.

Pappenberger, F., Frodsham, K., Beven, K., Romanowicz, R., Matgen, P., 2007. Fuzzy set approach to calibrating distributed flood inundation models using remote sensing observations. Hydrol. Earth Syst. Sci. 11, 739–752.

Plaza, D. A., De Keyser, R., De Lannoy, G. J. M., Giustarini, L., Matgen, P., Pauwels, V. R. N., 2012. The importance of parameter resampling for soil moisture data assimilation into hydrologic models using the particle filter. Hydrol. Earth Syst. Sci. 16 (2), 375–390.

Smith, P., Hughes, D., Beven, K., Cross, P., Tych, W., Coulson, G., Blair, G., 2009. Towards the provision of site specific flood warnings using wireless sensor networks. Meteorol. Appl. 15 (1), 57–64.

Smith, P. J., Beven, K. J., Tawn, J. A., 2008. Detection of structural inadequacy in process-based hydrological models: A particle-filtering approach. Water Resour. Res. 44, W09403.

USACE, 2002. United States Army Corps of Engineers: Theoretical basis for one-dimensional flow calculations. In: Hydraulic reference manual. USACE, Davis (CA, USA), Ch. 2, version 3.1. URL http://www.hec.usace.army.mil/software/hec-ras/

Watson, C., Coleman, R., Handsworth, R., 2008. Coastal tide gauge calibration: A case study at macquarie island using gps buoy techniques. Journal of Coastal Research 24 (4), 1071–1079.

Yoon, Y., Durand, M., Merry, C. J., Clark, E. A., Andreadis, K. M., Alsdorf, D. E., 2012. Estimating river bathymetry from data assimilation of synthetic swot measurements. J Hydrol 464–465 (0), 363 – 375.